SUPPORTING INFORMATION

S1. Uncertainty analysis of the sediment depth estimations

This section describes the propagation of uncertainties to analyse the accuracy of sediment depth estimations with the temperature-based method developed in this study. For this purpose, we first identified the sources of uncertainty related to the estimation of sediment depths. We distinguished 4 types of uncertainty sources:

- **Passive temperature measurements**

This group includes measurements from temperature sensors located at the bottom of the sediment layer, at the sediment-water interface, and outside the lab-scale setup. The uncertainty of the temperature measurements is conditioned by the uncertainty of the sensor itself and by its calibration. The sensors were calibrated using the recirculating water bath, which provided a measurement stability of ±0.01 ºC according to specifications. Five temperature conditions were set between 15 ºC and 35 ºC, which were used to define linear relationships between the standard temperature of the water bath and the temperature measurements of each sensor. The complete calibration process is described in the experiment database.[1]

The uncertainty of the temperature measurements was calculated using the law of propagation of uncertainties (or Type B method). For this purpose, an intermediate step was required to calculate the uncertainties and covariance of the regression coefficients using ordinary least squares (OLS) regression.[2] As a safety factor, the maximum uncertainty value was chosen among all sensors, $u(T) = 0.0315\ °C$.

- **DPHP system**

This group includes the thermal properties of the sediments: thermal conductivity (k_t) and volumetric thermal capacity (C_v). These values were obtained by measuring the increase and subsequent recovery of temperature (T) in response to the heat pulse per unit length (q) introduced by the heater. In addition, we needed to measure the distance between the sensor and the heater (d) and the geometry of the heating resistor: diameter (D) and length (L).

The temperature sensor of the DPHP system was calibrated together with the passive temperature sensors. For this reason, the value obtained in the previous section was also used to define the uncertainty of the temperature measurements of the DPHP system. Regarding the uncertainty of the heat pulse per unit length, we also used the law of propagation of uncertainties. The heat pulse per unit length is defined as follows:

$$q = \frac{V \cdot I}{L} \cdot pwm \tag{S1}$$

where V is the voltage (volts), I is the current (A), L is the heating resistor length (m), and pwm is the pulse width modulation. The values corresponding to these parameters were: $V = 11.96\ volts$, $I = 2\ A$, $L = 0.046\ m$. In addition, a value of $pwm = 0.3$ was established, which implies that the heat pulse is active 30 % of the time. This value ensured that the heat pulse was long enough to estimate thermal properties without causing sediment overheating, which could lead to biological reactions. As V, I, and L are independent terms, there is no covariance between them and therefore the uncertainty of the heat pulse per unit length can be expressed as:

$$u(q)^2 = u(V)^2 \cdot \left(\frac{\partial q}{\partial V}\right)^2 + u(I)^2 \cdot \left(\frac{\partial q}{\partial I}\right)^2 + u(L)^2 \cdot \left(\frac{\partial q}{\partial L}\right)^2 \quad \text{(S2)}$$

$$\frac{\partial q}{\partial V} = \frac{I}{L} \cdot pwm \quad \text{(S3)}$$

$$\frac{\partial q}{\partial I} = \frac{V}{L} \cdot pwm \quad \text{(S4)}$$

$$\frac{\partial q}{\partial L} = -\frac{V \cdot I}{L^2} \cdot pwm \quad \text{(S5)}$$

where $u(V)$, $u(I)$, $u(L)$ are the standard uncertainties of the voltage, current and heating resistor length, respectively. Note that pwm is a constant coefficient, and therefore its uncertainty is neglected.

$u(V)$ was obtained from the maximum deviation of the voltage measurement in the printed circuited board (PCB), resulting in $u(V) = 0.014\ volts$. In addition, a 3% deviation of the current was considered for the definition of $u(I)$, following the specifications of the AC-DC adaptor manufacturer. This resulted in $u(I) = 0.06\ A$. Finally, $u(L)$ was influenced by the instrument for measuring the heater length, for which a Vernier Caliper with a resolution of 1/20 mm was used. The measurement process with a Vernier Caliper is typically defined as the difference between the scales corresponding to the two ends of the object, i.e., $L = L_0 - L_1$, where L_0 and L_1 correspond to the initial and final scales. The uncertainty of each scale is associated with the resolution of the Vernier Caliper and was assumed to be $u(L_0) = u(L_1) = 0.1\ mm$. Thus, we can express $u(L)$ by applying the law of propagation of uncertainties, $u(L) = \sqrt{0.1^2 + 0.1^2} = 0.14\ mm$. As a result, the uncertainty of the heat pulse per unit heat was $u(q) = 4.71\ W/m$.

Regarding the distance between the heater and the temperature sensor, the uncertainty of the measurement was the same as for the heater length because the same measuring device was used. Finally, the uncertainty of the heating resistor diameter was estimated according to the manufacturer's specifications. The reference for the heating resistor diameter inside the cartridge

was 4 mm. However, due to the unknown measurement method used, a uniform probability distribution of the diameter was considered: $U(3.5,4.5)$.

As direct calculations with the law of propagation of uncertainties (Type B method) is not convenient, the Monte Carlo method (MCM) was applied to obtain the uncertainties of the thermal properties, i.e., $u(k_t)$ and $u(C_v)$. For this purpose, each DPHP measurement was computed repeatedly by assigning a normal distribution to the previous parameters, except for the heating resistor diameter, for which a uniform distribution was considered. At least three measurements were performed with the DPHP system in each test to estimate the sediment thermal properties. Consequently, the maximum values of $u(k_t)$ and $u(C_v)$ were considered for the subsequent analysis of the uncertainties of the sediment depth estimations.

- **Convective heat transfer coefficient**

The convective heat transfer coefficient (h) was estimated from the fit of the experimental and simulated temperature series at the sediment-bed. The simulated sediment-bed temperatures were computed with the diffusion heat transfer equation by considering the value of the sediment depth from the graded system and the mean k_t and C_v values from each experiment. Thus, h was the only unknown parameter. A fitting model was programmed in MATLAB by establishing the minimum value of the root mean square error (RMSE) between the experimental and simulated sediment-bed temperatures as the objective function.

Figure S1 shows the best fitting h-values for each experiment. As a result, $h = 1.75\ W/m^2/°C$ was obtained as a mean value, similar to those reported for plastic materials.[3] However, h-values showed a significant oscillation between 1 and 2.5 W/m2/ºC. For this reason, a uniform distribution $U(1.0,2.5)$ was considered for the subsequent analysis of the uncertainties of the sediment depth estimations.

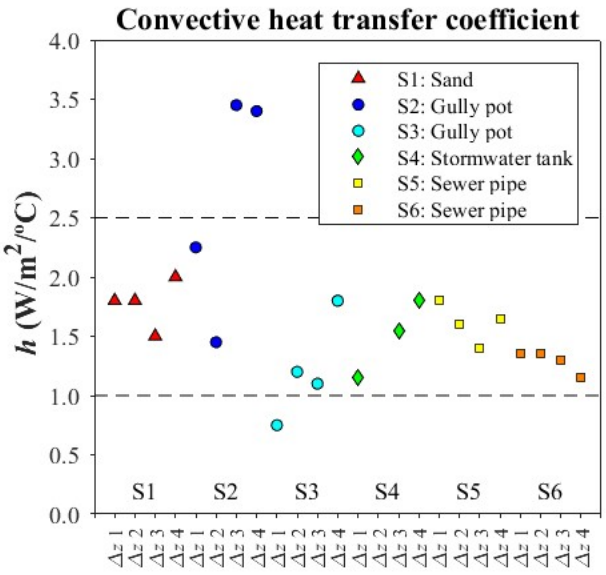

Figure S1. Convective heat transfer coefficients (h) that showed the best fit between the experimental and simulated sediment-bed temperatures.

- **Surrogate model**

The surrogate model was developed to obtain sediment depths from the harmonic features of the wastewater and sediment-bed temperature patterns, the sediment thermal properties and the bottom boundary condition. This model was developed by computing the nondimensional 1D diffusion heat transfer equation. For this purpose, we used field wastewater temperature measurements and wide ranges for the other input parameters, which covered the experimental conditions. Therefore, the model itself was a source of uncertainties because it was developed by using temperature measurements.

The field temperature time series were measured with the same type of sensors as used in the lab-scale model. Therefore, the same uncertainty was assumed. The MCM was applied to propagate the uncertainty of the temperature series in the wastewater to obtain the uncertainty of the harmonic features, i.e., amplitude ratio $u(A_r)$ and phase difference $u(\Delta\phi)$. Figure S2 shows the relationship between the nondimensional parameters $\Delta\chi$ and $\hat{\alpha}$, and the uncertainty of the harmonic features. The uncertainty increases for large sediment depths and leakage coefficients (bottom boundary condition). The increase of $u(A_r)$ and $u(\Delta\phi)$ for large depths is caused by the large attenuation of the sediment-bed temperature series compared to the wastewater temperature and, subsequently, a high uncertainty of the harmonic features could be expected.

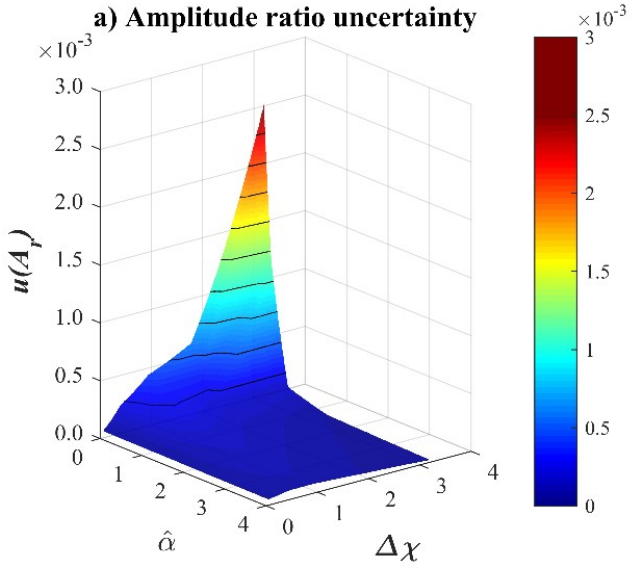

Figure S2. cont.

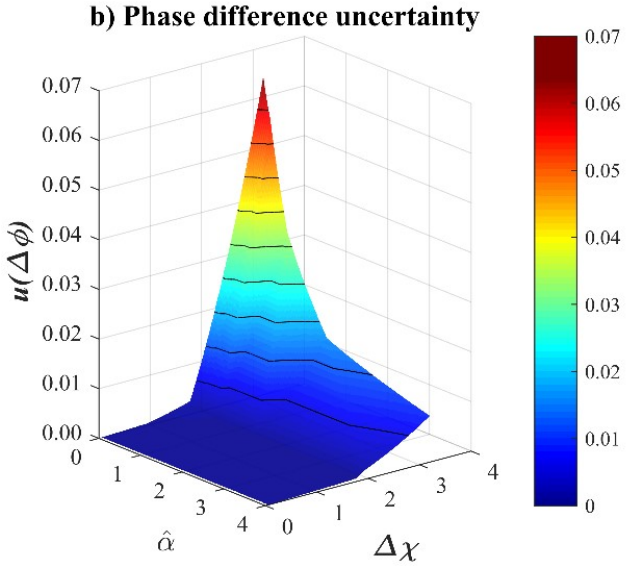

Figure S2. (a) Amplitude ratio and (b) phase difference uncertainties in the domain of the nondimensional parameter ($\Delta\chi$ and $\hat{\alpha}$).

Once all contributing uncertainty sources were identified and quantified, the MCM was performed to determine the uncertainty of the sediment depths estimated with the temperature-based system in the lab-scale model. Table S1 summarizes the probability distributions assumed for each of the parameters. Most parameters were described by a normal distribution (which is usually relevant for measured quantities) except for the convective heat transfer coefficient as it was not directly measured.

Table S1. Summary of the uncertainty sources, parameters, and probability distributions assumed in the MCM performed to estimate the uncertainty of the sediment depth estimations.

Uncertainty source	Parameter	Probability distribution
Passive temperature measurements	Water temperature, T_w (ºC)	Normal distribution, $N(T_w,0.0315)$
	Sediment-bed temperature, T_s (ºC)	Normal distribution, $N(T_s,0.0315)$
	Contour temperature, T_∞ (ºC)	Normal distribution, $N(T_\infty,0.0315)$
DPHP system	Thermal conductivity, k_t (W/m/ºC)	Normal distribution, $N(\bar{k}_t,max(u(k_t)))$
	Volumetric heat capacity, C_v (MJ/m^3/ºC)	Normal distribution, $N(\bar{C}_v,max(u(C_v)))$
Convective heat transfer coefficient	Convective heat transfer coeff., h (W/m^2/ºC)	Uniform distribution, $U(1.0,2.5)$
Surrogate model	Amplitude ratio, A_r (-)	Normal distribution, $N(A_r,f(\Delta\chi,\hat{\alpha}))$
	Phase difference, $\Delta\phi$ (-)	Normal distribution, $N(\Delta\phi,f(\Delta\chi,\hat{\alpha}))$

Figure S3 shows the results of the uncertainty propagation of the sediment depth estimations, using the MCM with a sample size of 106. Small sediment depths show non-symmetric distributions, whereas large values tend to show normal distributions. The lower part of the distribution dominates at the first or second sediment depth levels ($^{\Delta z_1}$ and $^{\Delta z_2}$). These differences are caused by the combination of different probability distributions. Most of the distributions of the parameters were uniform, except for the leakage coefficient, whose distribution was influenced by the uniform distribution assigned to the convective heat transfer coefficient (^{h}). As a result, we can conclude that small sediment depths are sensitive to the bottom boundary condition. Conversely, the influence of the bottom boundary condition is negligible for large sediment depths. The same conclusion was obtained in the sensitivity analysis performed in Regueiro Picallo et al.[4]

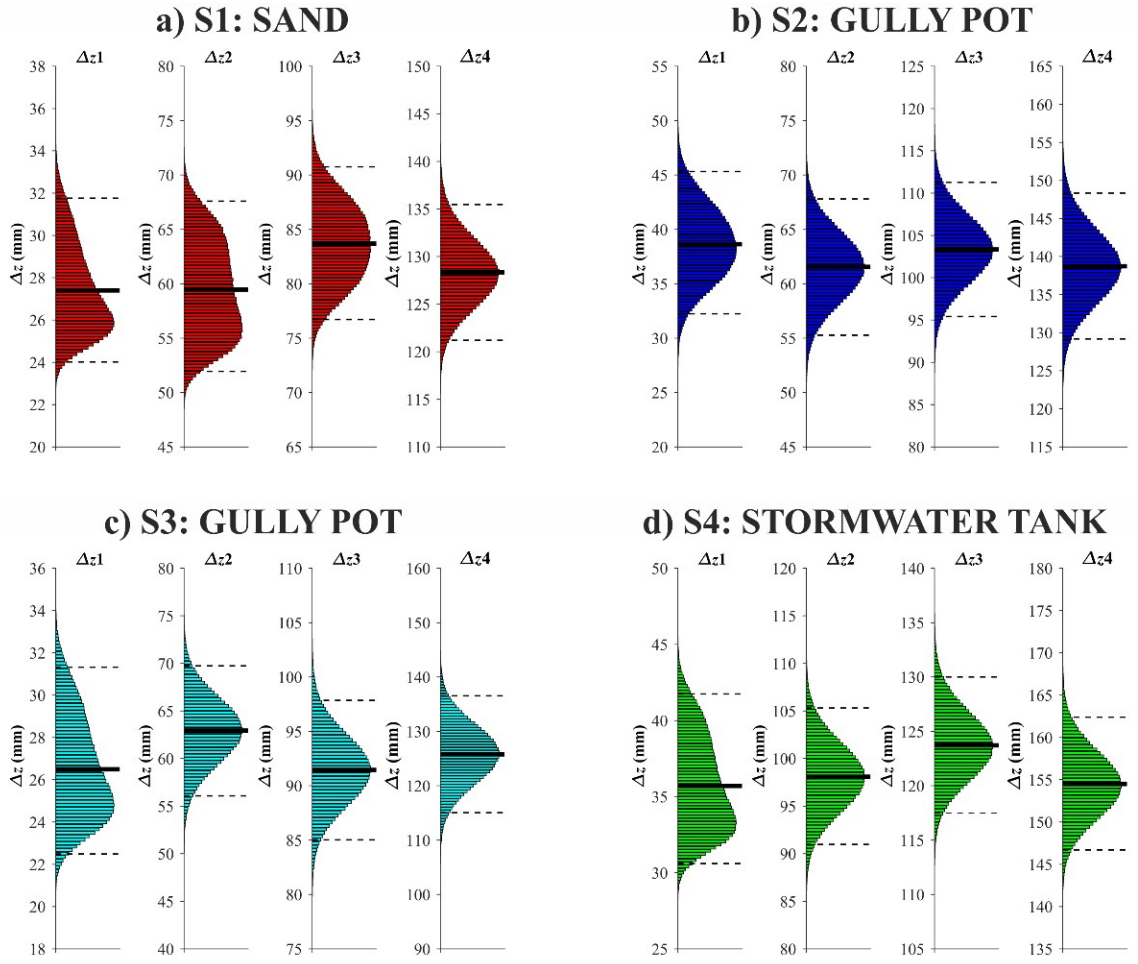

Figure S3. cont.

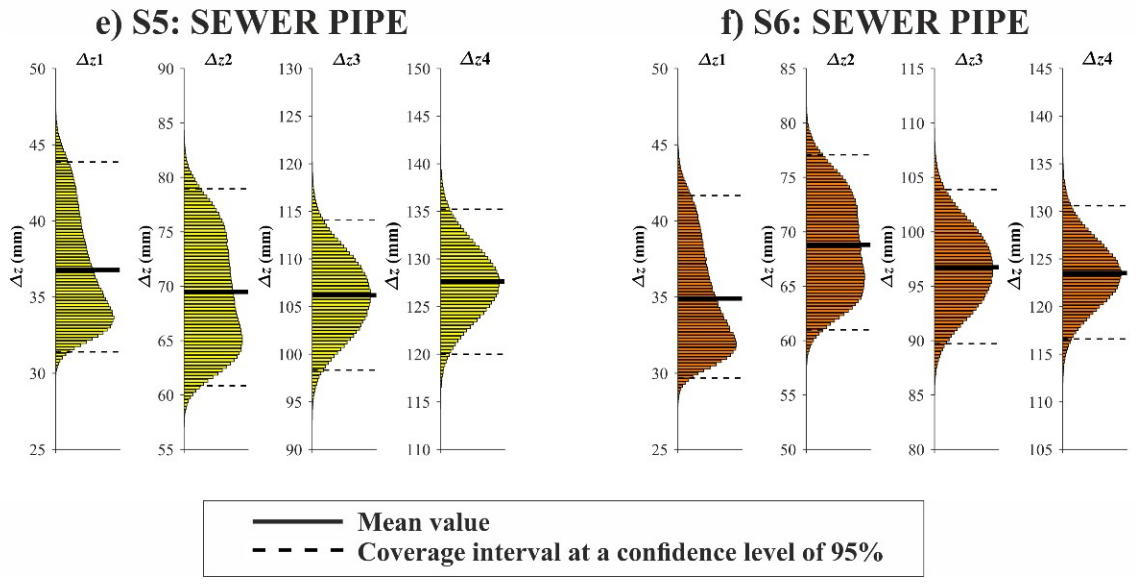

Figure S3. (a-f) Histograms resulting from the uncertainty propagation performed to the sediment depth estimations by the MCM.

S2. Influence of flow velocity at the top boundary in the heat transfer process

A fluid flowing over a surface generates shear stress, which triggers a convective heat transfer process. In the present study, the wastewater flow over the sediment bed accelerates heat transfer between both layers. A Dirichlet-type boundary condition was assumed at the top-boundary of the sediment-layer domain to simulate the 1D diffusion heat model and, subsequently, develop the surrogate model. However, a Cauchy-type condition would strictly reproduce the convective heat transfer processes at the water-sediment interface, similar to the bottom-boundary condition (Eq. 5). Therefore, the top-boundary condition of the 1D diffusion heat model was modified to evaluate the influence of the flow conditions:

$$-k_t \left.\frac{dT}{dz}\right|_{z0} = h_w(T_{z0} - T_w) \tag{S6}$$

where z denotes the vertical dimension (m), $z0$ the position of the water-sediment interface, T_{z0} is the sediment temperature at the top-boundary (ºC), T_w is the water temperature (ºC), and h_w is the convective heat transfer coefficient at the top-boundary (W/m²/ºC) that can be expressed as follows for a flat surface:

$$h_w = \frac{Nu_L k_{t_w}}{L} \tag{S7}$$

where L is the longitudinal dimension of the flat surface, i.e. pipe length (m), k_{t_w} is the thermal conductivity of the water, assumed to be $k_{t_w} = 0.598$ W/m/ºC, and Nu_L is the Nusselt number that can be expressed for turbulent flows in flat surfaces as follows:

$$Nu_L = 0.037 Re^{4/5} Pr^{1/3} \tag{S8}$$

where Re is the Reynolds number expressed as $Re = uL/\nu$, in which u is the flow velocity (m/s) and ν is the kinematic viscosity of the water (m²/s) assumed to be $\nu = 10^{-6}$ m²/s, and Pr is the Prandtl number expressed as $\Pr = \nu \rho_w c_{p_w} / k_{t_w}$, where ρ_w and c_{p_w} are the density (kg/m³) and the specific heat capacity (J/kg/ºC) of the water, respectively ($\rho_w = 997$ kg/m³ and $c_{p_w} = 4186$ J/kg/ºC).

Simulated sediment-bed temperatures were compared between 1D heat diffusion models including a Dirichlet- (Eq. 7) and a Cauchy-type (Eq. S6) condition respectively at the top-boundary to analyse the influence of the flow velocity on the heat transfer processes. The simulations of the sediment-bed temperatures were performed by simplifying the input variables. For this purpose, the UWO wastewater temperature series (Figure 2), the thermal properties of a sewer sample (sample S5) and the heat loss condition at the bottom-boundary ($h = 1.75$ W/m²/ºC)

were selected. In addition, a standard pipe length of 6 m was considered, although its value is barely sensitive to determine the convective heat transfer coefficient at the top-boundary ($h_w \propto L^{1/5}$). Consequently, the simulations were performed varying the flow velocity and the sediment depth. For this purpose, temperatures were simulated for a flow velocity range [0.1,0.4] m/s, which can lead to sediment accumulation,[5] and the same range of sediment depths used to develop the surrogated model Δz = [10,190] mm.

The root mean square error (RMSE) was computed to compare the simulated sediment-bed temperature series. Table S2 shows the maximum RMSE depending on flow conditions. The RMSE-values for low velocities of 0.1 m/s, for which a high accumulation rate is expected, were less than 0.009 ºC, while the RMSE was less than 0.005 ºC for flows higher than 0.2 m/s. The differences between the two models were negligible because the h_w-values in the model that considers convection at the top-boundary were very large ($h_w \geq 295$ W/m²/ºC). Therefore, a Dirichlet-type boundary condition can be assumed to simulated heat transfer processes at the water-sediment interface ($T_{z0} = T_w$) and, subsequently, the methodology does not depend on hydraulic variables, simplifying monitoring of sewer pipes.

Table S2. Simulated flow conditions with the heat transfer model including the Cauchy-type condition on the top-boundary and comparison of the simulated sediment-bed temperatures at the bottom of the domain: flow velocity (m/s), Reynolds and Nusselt numbers, convective heat transfer coefficient at the top-boundary (W/m2/ºC), and maximum RMSE (ºC).

u (m/s)	Re (-)	Nu_L (-)	h_w (W/m²/ºC)	max(RMSE) (ºC)
0.1	6×10^5	3.0×10^3	296	0.008
0.2	12×10^5	5.2×10^3	515	0.004
0.3	18×10^5	7.1×10^3	712	0.002
0.4	24×10^5	9.0×10^3	896	0.001

S3. Influence of the bottom boundary for determining the thermal properties

A comparative DPHP measurement was performed in a wide beaker to check that the distance from the heater to the bottom of the lab-scale model does not affect the measurement of the sediment thermal properties. Table S3 shows the values of k_t and C_v for each configuration.

Table S3. Saturated sand k_t and C_v measurements performed with the DPHP system at different locations: bottom of the lab-scale model and center of a beaker.

Thermal property	Lab-scale model	Beaker	|Relative error|
$k_t\ (W/m/ºC)$	1.374 ± 0.018	1.433 ± 0.010	4.1 %
$C_v\ (MJ/m^3/ºC)$	2.654 ± 0.027	2.786 ± 0.110	4.7 %

The relative error between the measurements is less than 5%. The distance from the heater to the bottom of the lab-scale model does not significantly influence the measurement of the thermal properties because the radial temperature distribution around the heater is small. The DPHP systems were developed to measure thermal properties by introducing short pulses that do not produce thermal inertia in the model. The TP01 sensor (Hukseflux, The Netherlands) selected to compare the thermal property measurements operates similarly. The manufacturer establishes a minimum distance 0.05 m at which the TP01 sensor must be buried in the sediment layer.[6]

S4. References

1. M. Regueiro-Picallo, J. Rieckermann, C. Ebi, S. Bloem and J. Langeveld, *Combining active and passive temperature signals for estimating sediment depths*, ZENODO, 2023. https://doi.org/10.5281/zenodo.8414446.
2. J. L. Bertrand-Krajewski, F. Clemens-Meyer and M. Lepot, *Metrology in urban drainage and stormwater management: Plug and pray*, IWA Publishing, London, UK, 2021. ISBN 9781789060119. Open Access available at https://doi.org/10.2166/9781789060119.
3. S. M. Koju, Thermal behaviour of expanded polystyrene based lightweight concrete sandwich panel at various temperatures. *J. Sci. Eng.*, 2017, **4**, 47-52. doi: https://doi.org/10.3126/jsce.v4i0.22381.
4. M. Regueiro-Picallo, J. Anta, A. Naves, A. Figueroa and J. Rieckermann, Towards urban drainage sediment accumulation monitoring using temperature sensors. *Env. Sci.: Water Res. Technol.,* 2023. https://doi.org/10.1039/d2ew00820c.
5. M. Regueiro-Picallo, J. Suárez, E. Sañudo, J. Puertas and J. Anta, New insights to study the accumulation and erosion processes of fine-grained organic sediments in combined sewer systems from a laboratory scale model, *Sci. Total Environ*., 2020, 716, 136923. https://doi.org/10.1016/j.scitotenv.2020.136923.

6. Hukseflux, User manual TP01: thermal properties sensor. Hukseflux, The Netherlands, 2023.